Generation of high conical angle Bessel-Gauss beams with reflective axicons

Pauline Boucher,[1,2] Jesus Del Hoyo,[3] Cyril Billet,[3] Olivier Pinel,[1] Guillaume Labroille,[1] and Francois Courvoisier[3,1,2,3]

[1)] *Laboratoire Kastler Brossel, Sorbonne Université, CNRS, PSL Research University, Collège de France, 4 Place Jussieu, 75005 Paris, France.*

[2)] *CAILabs, 38 boulevard Albert 1er, 35200 Rennes, France.*

[3)] *FEMTO-ST Institute, Univ. Bourgogne Franche-Comté, CNRS, 15B avenue des Montboucons, 25030 Besanon, cedex, France.*

We report the generation of Bessel-Gauss beams of high conical angle, up to 35 degrees, using reflective off-axis axicons and a magnification optical system. We experimentally characterize the beams with three-dimensional scans. The high precision of fabrication of the axicons in the vicinity of the axicon singularity allows us to generate a beam with intensity distribution close to analytical description.

I. INTRODUCTION

Diffraction-free Bessel beams were discovered by Durnin *et al* in 1987[1]. They are formed out of a conical interference of an infinite number of plane waves, crossing the optical axis at the same angle, here referred to as the *conical angle*. The constructive interference on the optical axis produces an intense central spot surrounded by several cylindrically-symmetric lobes with lower intensity. This beam structure is diffraction-free since its intensity profile is invariant with propagation. Obviously, finite energy beams preserve this structure only over a finite distance[2]. Bessel-Gauss beams are one of those finite energy realizations of Bessel beams. In a Bessel-Gauss beam, the interference is formed after a conical phase is applied on a Gaussian beam[3,4]. In this realization, the on-axis intensity profile evolves smoothly with a bell-shaped profile[2,4,5], in contrast with other forms of finite energy Bessel beams where the on-axis intensity oscillates, such as in the first realization by Durnin *et al*.

Bessel beams have found a variety of applications in optics. They are used as optical traps[6], for light-sheet microscopy[7,8], nonlinear optics and filamentation[9–11], for the guiding of electric discharges[12,13], material processing[14–17] or even for cellular transfection[18].

Bessel-Gauss beams are either produced from transmissive axicons (discovered well before the diffraction-free property[19]) or reflective Spatial Light Modulators (SLM). While the first enable shaping of higher power beams, the latter enable higher quality beams but at the cost of very low cone angles. Two difficulties arise in this field. On the one hand, the low conical angle values are compensated by telescopic magnification, but at the cost of a reduction in beam length by the square of the magnification if high angles are needed for applications. On the other hand, beam shaping with bulk glass axicons usually encounters another difficulty which is the processing of the tip, which cannot be infinitely sharp. The roundness produces a spherical wave which interferes with the Bessel beam. This generates deleterious oscillations of the on-axis intensity[20]. Several techniques have been developed to circumvent the impact of blunt tips, such as Fourier filtering[20] or using liquid immersion[21], but they are not energy efficient or easily implementable.

Here we report high quality Bessel-Gauss beam generation with reflective off-axis axicons where spatial filtering is unnecessary. These are compatible with high powers and produce cone angles sufficiently high that a magnification factor of only $\times 55$ is required to generate the highest conical angles ($35°$) produced to the best of our knowledge. This relatively low value of magnification also enables and generate Bessel beams with length exceeding 100 μm.

II. REFLECTIVE AXICONS

Our experimental setup is based on reflective axicons in oblique illumination to enable further use with high power lasers. In this case, it is necessary to engineer the surface to generate off-axis beams and avoid potential distorsion due to the oblique illumination[22]. The theoretical phase profile for the axicons we generated follows[23]: $\Phi(x,y) = (2\pi/\lambda)\tan\beta\sqrt{\cos^2(\alpha)x^2+y^2}$ where α is the incidence angle of the beam on the axicon, and $\beta = \theta/2$ where θ is the conical angle of the Bessel beam produced. The factor 1/2 simply arises from the reflection which doubles the optical path. The axicons were produced by lithography from a metallic substrate which has been coated by a broadband reflective dielectric coating at a central wavelength of 800 nm for further use with high power femtosecond Ti:Sapphire lasers. Three different axicons with different conical angles were produced and tested, with angles: $\theta_1^{'} = 3.842$ mrad, $\theta_2^{'} = 4.546$ mrad and $\theta_3^{'} = 5.215$ mrad. After magnification of 1/55, as we will see later, these axicons allowed us to produce Bessel-Gauss beams with conical angles of, respectively : $\theta_1 = 25$, $\theta_2 = 30$ and $\theta_3 = 35$. Figure 1(a) shows the difference between the theoretical profile of the "on-" and "off-" axis axicons corresponding to the cone angle of θ_1 ($\alpha = 5°$).

In Fig. 1(b), we show the surface roughness characterization by interferometry and its comparison with the theoretical profile. In particular, we plot in the inset a magnified view around the tip. We observe that the size of the region exhibiting a significant profile difference from the theoretical profile is smaller than 50 μm. This was also the case for the other 2 axicons produced.

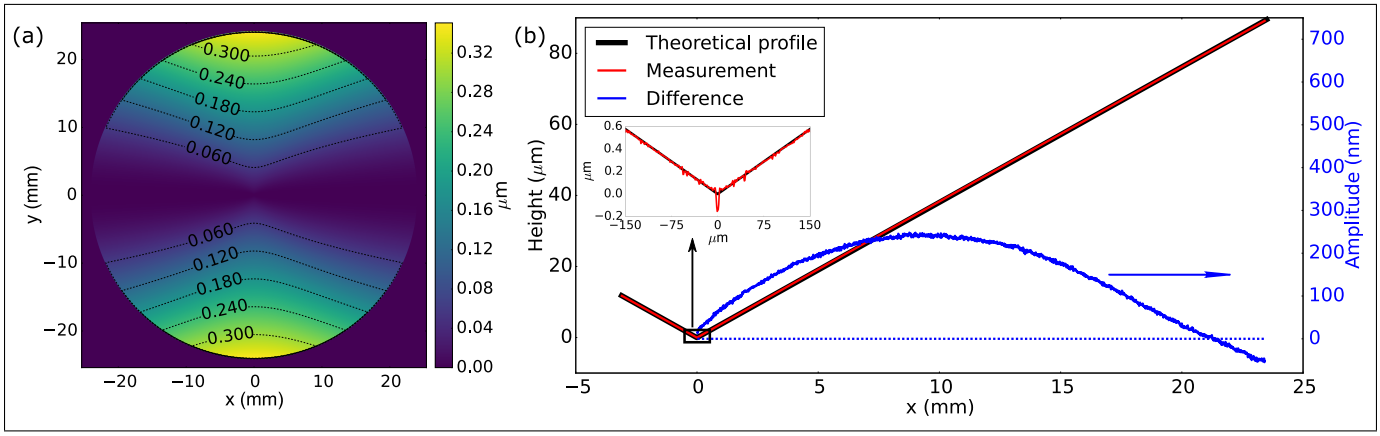

FIG. 1. Characterization of axicon $\theta_1^{'} = 3.842$ mrad. (a) Difference between an "on-axis" axicon and the off-axis axicon produced. (b) Comparison between theoretical and measured axicon profiles.

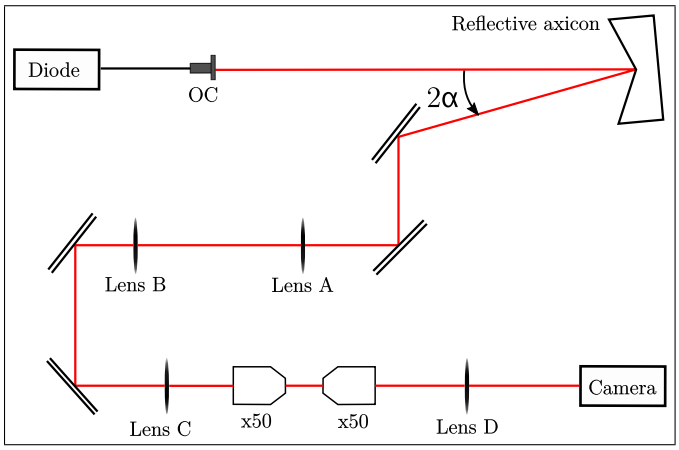

FIG. 2. Experimental setup (OC: output coupler). Lens A and lens B make up the first telescope and have focal lengths f_A=200 mm and f_B = 400 mm. Lens C and lens D have focal lengths f_C = 400 mm and f_D = 200 mm. The pixel pitch of the camera is 4.65 μm.

III. EXPERIMENTAL SETUP

We tested the axicons one by one using the same experimental setup, which is shown in figure 2. The optical source is a laser diode with central wavelength $\lambda = 780$ nm. The input beam is a single mode Gaussian beam with a waist (radius at $1/e^2$) $w_0 \sim 3$ mm. The optical path was carefully adjusted so that the axicon illumination angle is precisely $\alpha = 5°$. After incidence on the axicon, the beam is magnified by two successive confocal telescopes, with magnifications factors respectively $\gamma_1 = 2$ and $\gamma_2 = 1/110$ in order to produce a total magnification of $\gamma = 1/55$. The produced beam was then imaged onto a CCD camera with an imaging system of magnification $\times 56$ combining a $\times 50$ microscope objective with 3.6 mm focal length and a lens of focal length 200 mm. The imaging microscope objective was mounted on a motorized translation stage so as to scan across the Bessel beam we generated.

IV. RESULTS

In Fig. 3, we plot our results for the three different axicons used. For each Bessel-Gauss beam, we represented the cross section (x,y) of the transverse intensity profile at the propagation distance corresponding to the peak of intensity and a cross-section (x,z) of the longitudinal intensity profile. In all three cases, the high quality of the beam is apparent. Only a minor deviation from perfect circular symmetry of the transverse profile is observed and attributed to a small misalignement. Table I summarizes the experimental beam parameters.

TABLE I. **Theoretical beam parameters**

Conical angle	Central lobe diameter (FWHM)	Bessel zone length (measured at FWHM)
25	0.67 μm	130 μm
30	0.58 μm	110 μm
35	0.51 μm	95 μm

The evolution of the on-axis intensity with propagation distance is an important parameter qualifying the quality of the Bessel-Gauss beam. In Fig. 4, we compare the on-axis intensity $I(r = 0, z)$ of the beams, shown as black curve with the theoretical profile (red curve) obtained from stationary phase approximation of the diffraction integral[4,15]: $I(z) = 8\pi P_0 z \sin^2\theta/(\lambda w^2) \exp\left[-2(z\sin\theta/w)^2\right]$. θ is the conical angle, $w = 3187\mu$m is the waist of the incident Gaussian beam (value obained by fitting the experimental results), and P_0 is the input peak power. We compared the normalized profiles. An excellent agreement is found between experimental data and the analytical description of Bessel-Gauss beams.

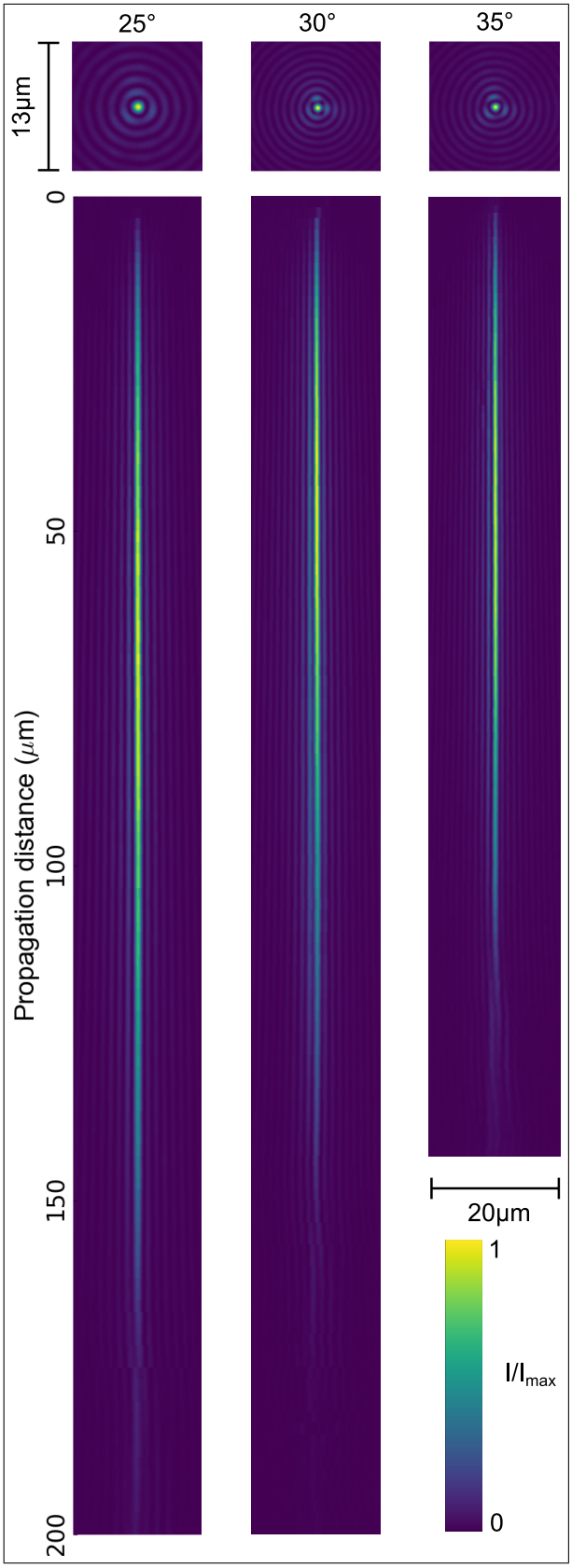

FIG. 3. Experimental images of transverse energy distribution and cross section of beams of 25, 30 and 35 conical angles.

We note that commercially available transmission axicons present a larger deviation from the perfect axicon because of the manufacturing of the tip of the axicon. In Fig. 4(a), we compare the profile obtained with a glass transmissive convex axicon with angle 0.5° (from Thorlabs) associated to a magnification system of 1/110 with the same input Gaussian beam. The generated conical angle is $\theta = 26°$, thus comparable to the first axicon. We observe that the on-axis intensity profile exhibits much larger deviations to the Bessel-Gauss profile expression, which is attributed to its blunt tip.

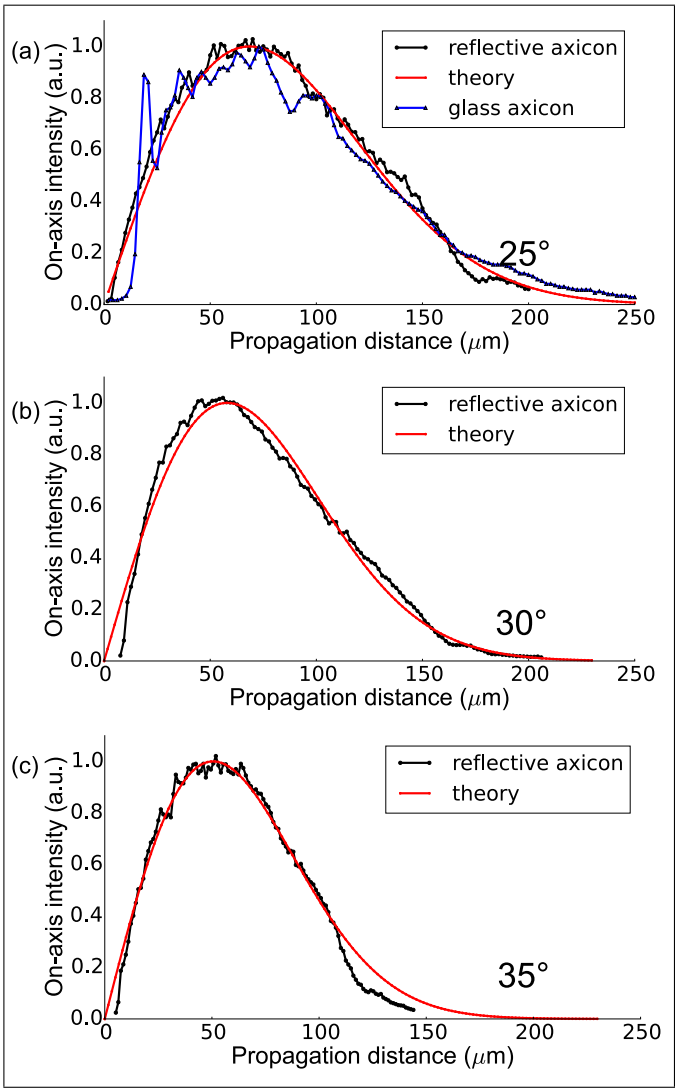

FIG. 4. (a) 25 conical angle: comparison between the on-axis intensity evolution along z for a glass axicon in transmission (blue, triangles), a reflective axicon (black, disks) and the theoretical profile for Bessel-Gauss beam of the same conical angle (red). (b) 30 and (c) 35 conical angles: comparison between the measured on-axis intensity evolution and the analytical description of the on-axis intensity associated with such conical angles.

V. CONCLUSION

In conclusion, we have demonstrated experimental generation of high quality Bessel-Gauss beams with high conical angles, up to 35°. We used reflective off-axis axicons exhibiting high surface quality in excellent agreement with the target surface profile and with a very reduced imperfect zone around the axicon singularity. We anticipate that these results will enable novel applications for high-power ultrafast optics, such as nonlinear optics or laser micromachining.

VI. FUNDING INFORMATION

The research leading to these results has received funding from the European Research Council (ERC-CoG-682032-PULSAR). This work has been performed in cooperation with the Labex ACTION program, contract ANR-11-LABX-0001-01 and was partly supported by the French RENATECH network.

[1] J. Durnin, J. J. Miceli, and J. H. Eberly, Phys. Rev. Lett. **58**, 1499 (1987).
[2] D. McGloin and K. Dholakia, Contemporary Physics **46**, 15 (2005).
[3] F. Gori, G. Guattari, and C. Padovani, Optics Communications **64**, 491 (1987).
[4] V. Jarutis, R. Paškauskas, and A. Stabinis, Optics Communications **184**, 105 (2000).
[5] T. Čižmár and K. Dholakia, Opt. Express **17**, 15558 (2009).
[6] E. Mcleod and C. B. Arnold, Nature Nanotechnology **3**, 413 (2008).
[7] F. O. Fahrbach, P. Simon, and A. Rohrbach, Nature Photonics **4**, 780 (2010).
[8] T. A. Planchon, L. Gao, D. E. Milkie, M. W. Davidson, J. A. Galbraith, C. G. Galbraith, and E. Betzig, Nature Methods **8**, 417 (2011).
[9] E. Gaizauskas, E. Vanagas, V. Jarutis, S. Juodkazis, V. Mizeikis, and H. Misawa, Optics Letters **31**, 80 (2006).
[10] D. E. Roskey, M. Kolesik, J. V. Moloney, and E. M. Wright, Opt. Express **15**, 9893 (2007).
[11] D. Faccio, E. Rubino, A. Lotti, A. Couairon, A. Dubietis, G. Tamošauskas, D. G. Papazoglou, and S. Tzortzakis, Phys. Rev. A **85**, 033829 (2012).
[12] M. Scheller, N. Born, W. Cheng, and P. Polynkin, Optica **1**, 125 (2014).
[13] M. Clerici, Y. Hu, P. Lassonde, C. Milian, A. Couairon, D. N. Christodoulides, Z. Chen, L. Razzari, F. Vidal, F. Legare, D. Faccio, and R. Morandotti, Science Advances **1**, e1400111 (2015).
[14] A. Marcinkevi\vcius, S. Juodkazis, S. Matsuo, V. Mizeikis, and H. Misawa, Jpn. J. Appl. Phys. **40**, L1197 (2001).
[15] M. K. Bhuyan, F. Courvoisier, P. A. Lacourt, M. Jacquot, R. Salut, L. Furfaro, and J. M. Dudley, Applied Physics Letters **97**, 081102 (2010), https://doi.org/10.1063/1.3479419.
[16] M. Duocastella and C. Arnold, Laser & Photonics Reviews **6**, 607 (2012).
[17] F. Courvoisier, R. Stoian, and A. Couairon, Optics Laser Technology **80**, 125 (2016).
[18] X. Tsampoula, V. Garceés-Chavez, M. Comrie, D. J. Stevenson, B. Agate, C. T. A. Brown, F. Gunn-Moore, and K. Dholakia, Appl. Phys. Lett. **91**, 053902 (2007).
[19] J. H. McLeod, Journal of the Optical Society of America **44**, 592 (1954).
[20] O. Brzobohatý, T. Cižmár, and P. Zemánek, Opt. Express **16**, 12688 (2008).
[21] S. Akturk, C. L. Arnold, B. Prade, and A. Mysyrowicz, Optics Communications **282**, 3206 (2009).
[22] Z. Bin and L. Zhu, Applied Optics **37**, 2563 (1998).
[23] A. Thaning, Z. Jaroszewicz, and A. T. Friberg, Appl. Opt. **42**, 9 (2003).